

Thermal Magnetic Fluctuations and Anomalous Electron Diffusion

A. T. Lin and J. M. Dawson

Center for Plasma Physics and Fusion Engineering, University of California, Los Angeles, California 90024

and

H. Okuda

Plasma Physics Laboratory, Princeton University, Princeton, New Jersey 08540

(Received 19 June 1978)

We investigate electron transport for a thermal plasma using a magnetostatic plasma model. Three cases are investigated; (1) fixed ions, only magnetic fluctuations; (2) fixed ions, magnetic and electrostatic fluctuations; (3) mobile ions, magnetic, and electrostatic fluctuations. For (1), magnetic islands as well as many unclosed field lines occurred; for (2) and (3) electrostatic convective cells occurred along with magnetic islands giving a much more turbulent situation. Generally the transport due to electrostatic convective cells dominated.

Anomalous plasma diffusion due to thermally excited convective cells has been studied in detail.¹ Even for thermal equilibrium, plasma diffusion across a strong magnetic field can be dominated by zero-frequency fluctuations (convective cells). It has recently been pointed out² that in addition to the electrostatic convective cells, zero-frequency magnetic fluctuations exist in a two-dimensional situation which produce random magnetic islands as well as many open field lines for a shearless zero-order magnetic field. Since the particles can follow the magnetic field they can diffuse across the system; it is important to compare this diffusion with collisional diffusion and convective cell diffusion. Furthermore, since the motion of charged particles due to the convective cells can destroy the current filaments responsible for the magnetic fluctuations, a strong coupling between the electrostatic and magnetostatic fluctuations is expected to occur. This coupling should determine the correlation time of the thermal magnetic fluctuations. It is also possible for the fluctuating magnetic fields to give rise to shorting of the charges associated with the convective cells and affect their lifetime. This effect is only important at high β .

In order to study the above processes in detail, a set of two-and-one-half-dimensional simulations have been carried out using a magnetostatic particle code with a uniform external magnetic field in the z direction.³ The simulation parameters were the following: a 64×64 grid, 4096 ions and electrons, $\Omega_e/\omega_{pe} = 1$ (electron gyrofrequency/plasma frequency), $m_i/m_e = 36$, $T_e/T_i = 2$, $\lambda_{De}/\delta = 1$ (electron Debye length/grid spacing), $V_{Te}/c = \frac{1}{10}$ (electron thermal speed/speed

of light) and, $\beta = 0.04$ (plasma pressure/magnetic pressure); note that $\beta \approx m_e/m_i$ here.

To study the particle diffusion and the coupling between the electrostatic and magnetostatic fluctuations in detail, simulations are carried out in three steps. First, all the electrostatic fluctuations are suppressed in the code and the ions are treated as a stationary background (case 1). This will correspond to the case considered in Ref. 2. In Fig. 1, test-particle diffusion $\langle(\Delta x)^2\rangle$ with time is shown. We observe that $\langle(\Delta x)^2\rangle$ increas-

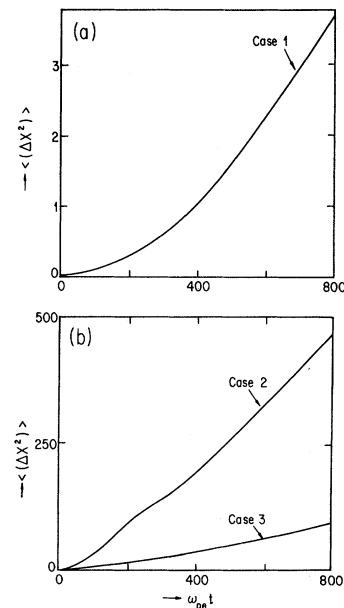


FIG. 1. Test-particle diffusion $\langle(\Delta x)^2\rangle$ vs time for (a) fixed ions, only magnetic fluctuations (case 1); (b) fixed ions, magnetic and electrostatic fluctuations (case 2); mobile ions, magnetic and electrostatic fluctuations (case 3).

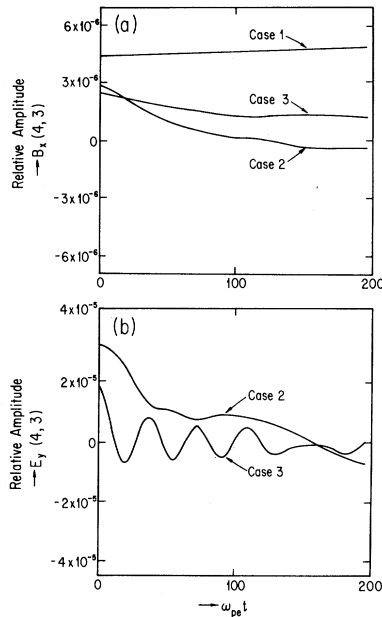


FIG. 2. Correlation function of the (4,3) mode of (a) the magnetic fluctuations B_x for three cases and (b) the electrostatic fluctuation E_y for two cases.

es as t^2 for a long time. The particle diffusion and the damping of the Fourier modes of magnetic fluctuations determined by measuring the correlation are quite small, as shown in Fig. 2(a). This is because without electrostatic fields, almost no damping mechanism exists for the magnetic fluctuations as predicted by the linear fluid theory which gives²

$$\omega = -i \frac{\nu_{ei} + k_{\perp}^2 \mu_e}{1 + \omega_{pe}^2 / c^2 k_{\perp}^2}, \quad (1)$$

where ν_{ei} is the electron-ion collision frequency and μ_e is the electron viscosity. The long-lived (coherent) magnetic fluctuations caused $\langle(\Delta x)^2\rangle$ to increase as t^2 . Measurements of the frequency spectrum confirm the presence of dc magnetic fluctuations as predicted by the linear theory and we observe many unclosed field lines as well as randomly situated magnetic islands which move very slowly across the main magnetic field (Fig. 3). Since the damping of the magnetic fluctuations is so small, nonlinear effects due to the coupling to the electrostatic convective cells can become dominant in determining the lifetime of the magnetic fluctuations.

To study the more realistic situations and in particular to confirm the strong coupling to the electrostatic convective cells, electrostatic fluctuations

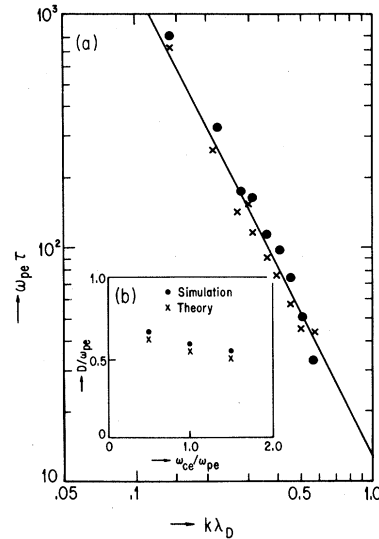


FIG. 3. (a) Decorrelation time for various Fourier modes of B_x (crosses) and E_y (solid dots). Note that both E_y and B_x decay as k^2 indicating the strong coupling between convective cells and magnetic fluctuations. (b) The diffusion rate vs the magnetic field strength.

are now allowed in the code while the ions are kept as a neutralizing uniform background (case 2). Note that in addition to the magnetic fluctuations, the upper hybrid oscillations and electrostatic convective cells come into play in the nonlinear evolution of the system. Enhanced particle diffusion and the damping (decorrelation) of the magnetic fluctuations are immediately observed due to the electrostatic convective cells as shown in Figs. 1 and 2. The observed damping rate is more than one order of magnitude larger than the collisional damping rate. Particle diffusion is mostly from the electrostatic convective cells, which agrees well with the theoretical predictions.⁴ Measurements of the correlations confirm the presence of a strong coupling of the magnetic and electrostatic fluctuations which both decay as

$$\omega = \frac{-ik_{\perp}^2 D}{2(1 + \Omega_e^2 / \omega_{pe}^2)}. \quad (2)$$

Figure 4(a) confirms this for various k . We observe that the decorrelation time ($c = 5\nu_{Te}$, $\Omega_e = 1.5\omega_{pe}$) of the magnetic fluctuations is very close to that of the electrostatic fluctuations indicating the strong turbulent nature for these

modes. In particular, long-wavelength modes which satisfy $k_{\perp} c < \omega_{pe}$ damp much faster than predicted by (1) if ν and μ are computed from collisions. This damping is important in predicting particle diffusion due to magnetic fluctuations.

Figure 4(b) compares the electron diffusion rate determined from the simulation results (solid dots) with the theoretical prediction (crosses) for case 2. In this case the diffusion comes from convective cells and magnetic fluctuations:

$$D = D_C + D_M, \quad (3)$$

where¹

$$D_C = \frac{c}{B_0} \left[\frac{2T}{1 + \omega_{pe}^2 / \Omega_e^2} \right]^{1/2} \left(\ln \frac{k_{\max} L}{2\pi} \right)^{1/2}$$

and²

$$D_M = \frac{\langle V_{\parallel}^2 \rangle^{1/2}}{B_0} (2T)^{1/2} \left[\ln \frac{k_{\max} L}{2\pi} - \frac{1}{2} \ln \frac{k_{\max}^2 + \omega_{pe}^2 / c^2}{(4\pi^2 / L^2 + \omega_{pe}^2 / c^2)^{1/2}} \right].$$

In the above expression, L is the system length and $\langle V_{\parallel}^2 \rangle^{1/2}$ is the thermal speed along the unperturbed field line. The simulations show that the diffusion rate has only a weak dependence on the magnetic field strength. This indicates that the diffusion is mainly due to convective cells while the diffusion process due to magnetic fluctuations should have a Bohm-like scaling.³⁻⁵

Finally simulations were carried out including the ion dynamics as well as all the fields (case 3). In addition to electrostatic convective cells, lower hybrid oscillations come into play for the determination of the electron diffusion and the correlation time. Particle diffusion and the correlation are shown in Figs. 1 and 2. We observe that the diffusion for this case is smaller than that for case 2 but much larger than that for case 1. The reduction is due to the fact that the ions reduce the flow velocity associated with the convective cell [$\langle V^2(k) \rangle = (4\pi T c^2 / B_0^2) (1 + \omega_{pi}^2 / \Omega_i^2 + \omega_{pe}^2 / \Omega_e^2)^{-1}$]. The electric field energy of the convective cells per mode for case 2 is given by $E_k^2 / 8\pi = (T/2) (1 + \omega_{pe}^2 / \Omega_e^2)^{-1}$ while it is given by $E_k^2 / 8\pi = (T/2) (1 + \omega_{pi}^2 / \Omega_i^2 + \omega_{pe}^2 / \Omega_e^2)^{-1}$ for case 3. A large part of electron diffusion for case 3 is caused by the lower hybrid oscillations which can cause a diffusion much larger than the convective cells and magnetic fluctuations even in a finite- β plasma ($\beta > m_e / m_i$). The measured diffusion for case 3 agrees reasonably well with the theoretical predictions due to lower hybrid oscillations.⁵

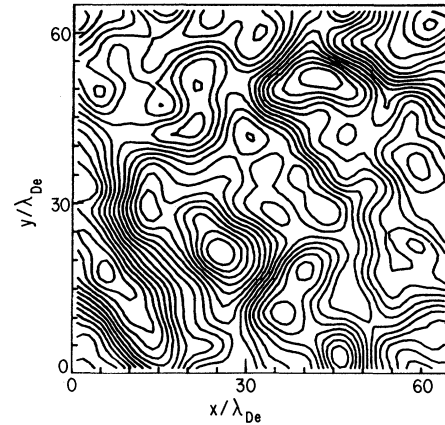


FIG. 4. The magnetic field lines projected on the $x-y$ plane at $\omega_{pe} t = 400$.

If we compare the electron diffusion due to magnetic fluctuations with the particle diffusion due to electrostatic convective cells, the former is larger than the latter for $\beta > m_e / m_i$. Note, however, that the convective diffusion gives rise to the ambipolar diffusion for both ions and electrons while only primarily electron diffusion is associated with the magnetic fluctuations. This diffusion is, however, much smaller than the electron self-diffusion due to lower hybrid oscillations.

We have examined only the simplest case, that of thermal equilibrium, to gain some understanding of the importance of magnetic fluctuations. For this case their effect is rather small. In a real plasma carrying current things may be different. In particular for plasmas near kink or other magnetic instabilities they may be more important. Magnetic fluctuations may also couple to other instabilities such as drift waves^{6,7} to produce enhanced magnetic fluctuations. On the other hand, magnetic shear tends to reduce the size of magnetic islands and reduce their influence on plasma transport. Much remains to be done in this area.

We would like to thank Mrs. Chi-Chien Lin for providing the numerical support. This work was supported by U. S. Department of Energy Contracts No. EY-76-C-03-0010 and No. EY-76-C-02-3073.

¹C. Chu, M. Chu, and T. Ohkawa, *Bull. Am. Phys. Soc.* **22**, 1135 (1977).

²J. M. Dawson, H. Okuda, and B. Rosen, in *Methods in Computational Physics*, edited by B. Alder *et al.* (Academic, New York, 1976), Vol. 16, p. 281.

³J. Busnardo-Neto, P. L. Pritchett, A. T. Lin, and J. M. Dawson, *J. Comput. Phys.* **23**, 300 (1977).

⁴Note that the diffusion due to convective cells may

be given by taking the limit $\omega_{pi} \rightarrow 0$ of the formula given by Ref. 1 since the ions do not participate for the determination of the convective cells.

⁵C. Chu, J. M. Dawson, and H. Okuda, *Phys. Fluids* **18**, 1762 (1975).

⁶C. Z. Cheng and H. Okuda, *Phys. Rev. Lett.* **38**, 708 (1976).

⁷J. D. Callen, *Phys. Rev. Lett.* **39**, 1540 (1977).

Observation of a Forbidden Line of Fe XX and Its Application for Ion Temperature Measurements in the Princeton Large Torus Tokamak

S. Suckewer and E. Hinnov

Plasma Physics Laboratory, Princeton University, Princeton, New Jersey 08540

(Received 10 July 1978)

A spectrum line in the Princeton Large Torus (PLT) tokamak discharges, with wavelength measured as $2665.1 \pm 0.3 \text{ \AA}$, has been identified as the $2s^2 2p^3 \ ^2D_{5/2} \rightarrow \ ^2D_{3/2}$ magnetic dipole transition in Fe XX ground configuration. A variety of localized spectroscopic diagnostics, e.g., ion temperature and density distribution measurements in the high-temperature interior of the plasma, are feasible by means of forbidden lines of this type. The 2665- \AA line has been used to measure near-central ion temperature in a discharge with auxiliary neutral-beam heating.

Special interest in forbidden lines of highly ionized atoms in plasma diagnostics arises for two reasons. One reason is that the radiation originates usually from a fairly localized region, where the ionization potential of the ion is roughly comparable to the local electron temperature. The other is that this radiation occurs at relatively long wavelengths, where optics (mirrors, perhaps windows and lenses) can be effectively used, thus allowing employment of versatile spectroscopic techniques. In the past, spectroscopic ion temperature and spatial distribution measurements in tokamaks have been restricted to the relatively abundant oxygen and carbon impurities,^{1,2} which become stripped and hence unobservable at temperature $\geq 0.7 \text{ keV}$.

In this paper, we report the first observation and diagnostic application of a Fe XX forbidden line in tokamak discharges. This line, from the transition $2s^2 2p^3 \ ^2D_{5/2} \rightarrow \ ^2D_{3/2}$ in the ground configuration, had not been directly observed before, although its approximate location was, of course, predictable. The wavelength (in air) was measured as $2665.1 \pm 0.3 \text{ \AA}$, corresponding to the 2D -level separation of $37511 \pm 4 \text{ cm}^{-1}$. The simple *LS*-coupling magnetic dipole radiative transition probability (which should be adequate to better than a factor 2) is 570 sec^{-1} . The identification of the line is based on the temporal and spatial variation of the observed emissivity in the dis-

charge, and the approximate agreement with the expected wavelength and intensity, as described below. Forbidden iron lines of Fe XXI at about 2300 and 1354 \AA have been also observed in the adiabatic toroidal compressor (ATC) and Princeton Large Torus (PLT) tokamaks, but not yet with sufficient intensity and reproducibility to allow accurate wavelength determination or consistent use for plasma diagnostics, mostly because of interfering radiation of other origin in the spectral neighborhood.

The energy levels and wavelengths of the ground configurations of Fe XX and neighboring iron ions are shown in Fig. 1. The energy levels and their scaling in isoelectronic sequences, and the observed lines, have been described by Edlen.^{3,4} The lines at 1354.1 \AA of Fe XXI, at 845.1 \AA of Fe XXII, and at 974.8 \AA of Fe XVIII have been observed in solar flares,⁵ the others are mostly deduced from differences of far-uv lines from laser-produced plasmas,^{6,7} or from *ab initio* calculations (except, of course, the coronal green line⁸ of Fe XIV). Magnetic dipole transition probabilities and wavelengths have been calculated by Cowan⁹ and Kastner, Bhatia, and Cohen.¹⁰ In general, the directly observed wavelengths are accurate to about $\pm 0.1 \text{ \AA}$, whereas the interpolated or calculated wavelengths are uncertain to at least several angstroms.

Figure 2 shows the temporal behavior of the